ARTICLE
Journal of Cellular Biochemistry 116:1101–1112 (2015)

Journal of Cellular Biochemistry

Heparan Sulfate D-Glucosaminyl 3-O-Sulfotransferase-3B1 (HS3ST3B1) Promotes Angiogenesis and Proliferation by Induction of VEGF in Acute Myeloid Leukemia Cells

Lei Zhang,[1] Kai Song,[1] Ling Zhou,[1] Zhishen Xie,[1] Ping Zhou,[1] Yiming Zhao,[2] Yue Han,[2] Xiaojun Xu,[1*] and Ping Li[1*]

[1]*State Key Laboratory of Natural Medicines, China Pharmaceutical University, Nanjing, China*

[2]*Jiangsu Institute of Hematology, Key Laboratory of Thrombosis and Hemostasis of Ministry of Health, The First Affiliated Hospital of Soochow University, Suzhou, China*

ABSTRACT

Heparan sulfate (HS) are complex polysaccharides that reside on the plasma membrane of almost all mammalian cells, and play an important role in physiological and pathological conditions. Heparan sulfate D-glucosamine 3-O-sulfotransferase 3B1 (HS3ST3B1) participates in the last biosynthetic steps of HS and transfers sulfate to the 3-O-position of glucosamine residues to yield mature sugar chains. To date very few biological processes or proteins have been described that are modulated by HS3ST3B1. In this study, we observed that HS3ST3B1 positively contributed to acute myeloid leukemia (AML) progression in vitro and in vivo, and these activities were associated with an induction of the proangiogenic factor VEGF expression and shedding. Moreover, the effects of HS3ST3B1 on VEGF release can be attenuated after treatment of heparanase inhibitor suramin, which prevented VEGF secretion and subsequently blocked VEGF-induced activation of ERK and AKT, suggesting that 3-O-sulfation of HS by HS3ST3B1 facilitated VEGF shedding; the effects of HS3ST3B1 on activation of ERK and AKT can also be blocked by VEGFR inhibitor axitinib, suggestive of a relationship between 3-O-sulfation of HS and VEGF-activated signaling pathways. Taken together, our findings support that VEGF is an important functional target of HS3ST3B1 and provide a new mechanism of HS3ST3B1 in AML. J. Cell. Biochem. 116: 1101–1112, 2015.

KEY WORDS: HEPARAN SULFATE (HS); HEPARAN SULFATE 3-O-SULFOTRANSFERASE-3B1 (HS3ST3B1); ACUTE MYELOID LEUKEMIA (AML); VEGF; ERK

Acute myeloid leukemia (AML) is a cancer of myeloid blood cells. When immature white blood cells (myeloblasts) lose the ability to differentiate, and/or gain mutations disrupting proliferation control, AML occurs, as manifested by uncontrolled growth of an immature clone of cells [Stone et al., 2004]. Also, increasing evidence points to the involvement of increased angiogenesis in this process [Dong et al., 2007]. Bone marrow (BM) provides important microenvironment for hematopoietic stem cells. Once AML cells enter BM, it induces angiogenesis by expressing receptors for angiogenic factor or secreting angiogenic factors, such as VEGF [Bellamy et al., 2001; Santos and Dias, 2004; Casalou et al., 2007]. In addition, previous studies demonstrated the expression of angiogenic factors endows AML myeloblasts the capability of proliferation, migration and resistance to chemotherapy [Dias et al., 2000; Casalou et al., 2007]. Therefore, identifying the modulators of angiogenic signaling would be a useful anti-AML strategy.

Heparan sulfate proteoglycans (HSPGs) have the complex structure and play the important role in tumorigenesis, tumor progression and metastasis [Sasisekharan et al., 2002]. The HSPG has two domains, the core protein and the heparan sulfate (HS) glycosaminoglycan chains linked on it. The glycosaminoglycan

Abbreviations used: HS3ST3B1, heparan sulfate 3-O-sulfotransferase-3B1; AML, acute myeloid leukemia; HSPG, heparan sulfate proteoglycans; VEGF, vascular endothelial growth factor; FBS, fetal bovine serum; HUVEC, human umbilical vein endothelial cell; CM, conditional medium; BM, bone marrow.

L. Zhang and K. Song contributed equally to this work.

Conflict of interest: The authors declare no conflict of interest.

*Correspondence to: Xiaojun Xu and Ping Li, State Key Laboratory of Natural Medicines, China Pharmaceutical University, No. 24 Tongjia Lane, Nanjing 210009, China.
E-mail: xiaojunxu2000@163.com (X.X.); liping2004@126.com (P.L.)

Manuscript Received: 25 December 2014; Manuscript Accepted: 18 December 2014

Accepted manuscript online in Wiley Online Library (wileyonlinelibrary.com): 23 December 2014

DOI 10.1002/jcb.25066 • © 2014 Wiley Periodicals, Inc.

chains are consisted of alternating units including N-acetylated or N-sulfated glucosamine and uronic acids (glucuronic acid or iduronic acid) [Bishop et al., 2007]. After the initial synthesis, HSPGs can be modified by a series of enzymes including the C5 epimerase, the 2-O-sulfotransferase, the 3-O- sulfotransferase and 6-O- sulfotransferase [Vanpouille et al., 2007].

Heparan sulfate modification of extracellular matrix proteins, as well as many secreted cytokines, such as fibroblast growth factor (FGF) and vascular endothelial growth factor (VEGF), largely change the activity of these proteins [Ferreras et al., 2012]. Highly sulfated HS domains, such as sulfates at 2-O-, 6-O-, and *N*-positions markedly facilitated VEGF dimerization and binding [Robinson et al., 2006]. The 3-O-sulfation is the rarest modification and it is accomplished by the 3-O-sulfotransferase (3ST), which has the largest family members in HS sulfotransferases [Lindahl et al., 1980; Shworak et al., 1997; Shworak et al., 1999]. However, the relationship between VEGF and the 3-O-sulfates of HS is still unclear. Our previous studies showed that HS3ST3B1 was associated with epithelial-mesenchymal transition during pancreatic cancer tumorigenesis [Song et al., 2011]. We also found that up-regulation of HS3ST3B1 expression was commonly observed in pancreatic cancer cell lines. However, the role of HS3ST3B1 in leukemia development remains unclear. In this study, we investigated the *in vitro* and *in vivo* functional roles of HS3ST3B1 in angiogenesis and leukemia tumorigenesis.

MATERIALS AND METHODS

CELL CULTURE AND ESTABLISHMENT OF HS3ST3B1 OVER-EXPRESSION AND KNOCKDOWN CELLS

The human acute myeloid leukemia cell line U937 (KeyGEN BioTECH) was cultured in RPMI 1640, supplemented with 10% fetal bovine serum (FBS), L-glutamine, and penicillin/streptomycin. U937 cells were transduced using an HIV-1-based lentiviral vector (LV) (GenePharma) carrying the green fluorescent protein gene and the full-length HS3ST3B1 cDNA. For the knockdown experiment, an LV carrying a HS3ST3B1-specific shRNA or a scrambled shRNA was transduced. Stable cell lines were selected with puromycin (1 μg/ml, Sigma). The HUVEC (human umbilical vein endothelial cell) line was obtained from the American Type Culture Collection and cultured in Dulbecco's modified Eagle's medium (DMEM), supplemented with 10% FBS, L-glutamine, and penicillin/streptomycin (all from Invitrogen).

CELL PROLIFERATION (MTT) ASSAY

A total of 2×10^4 cells from each of the stably transduced cell lines were seeded into 96-well tissue culture plates (100 μl complete medium without phenol red per well) and cultured with or without 300 μM suramin (Calbiochem), 100 ng/ml $VEGF_{165}$ (PeproTech), or 10 or 20 μM axitinib (Selleckchem). After 24 or 48 h, tetrazolium salt was added and the cells were incubated at 37 °C for another 4 h. The insoluble violet formazan product was solubilized by the addition of 10% SDS/5% isobutanol at 100 μl per well. The plates were read on a Biotek plate reader (Montpelier, Vermont) using a test wavelength of 570 nm.

COLONY FORMATION IN SOFT AGAR

Five hundred cells from each of the stably transduced cell lines were suspended in 1.2 ml of 0.35% (w/v) agar in RPMI 1640/20% FBS and overlaid onto 3 ml of 0.6% (w/v) agar in RPMI 1640/20% FBS in three wells of a 6-well plate. After 10 days, colonies with more than 30 cells were scored as positive using an inverted microscope.

PREPARATION OF CONDITIONED MEDIUM (CM) FROM STABLY TRANSDUCED CELLS

To analyze the influence of tumor microenvironment on leukemia cells, we collected CM from HS3ST3B1 over-expression or knock-down U937 cells after 48 h of incubation in RPMI 1640 medium with 1% FBS. The medium from the same numbers of cells was collected and centrifuged briefly to remove the cell debris.

SCRATCH ASSAY

To assess the mobility of HUVECs, a wound healing assay was performed. A total of 5×10^5 HUVECs were seeded in 6-well plates and incubated in FBS-free DMEM for 24 h. An artificial wound was then created, and the cells were washed and supplied with new growth medium of 50% DMEM containing 1% FBS and 50% CM. The migration of cells through the wound area was examined after 0, 6, 12 and 24 h.

TUBE FORMATION ASSAY

The HUVECs (2×10^4 cells per well) were seeded on top of matrigel-coated (50 μl per well) wells of 96-well tissue culture plates containing 150 μl complete DMEM and 150 μl CM per well. Tube formation was examined using a light microscope (Nikon, eclipse Ti-s, Tokyo, Japan) at 40 × magnification. Tube formation per area was analyzed using ImagePro Plus software.

ELISA

VEGF production was determined by enzyme-linked immunosorbent assay (ELISA) using a kit from R&D Systems according to manufacturer's instructions. Briefly, CM was collected from a culture of 7.5×10^5 stably transduced cells that have been incubated in RPMI 1640/1% FBS for 48 h. The CM was subjected to ELISA analysis and the final absorbance was measured at 450 nm.

REVERSE TRANSCRIPTION PCR AND QUANTITATIVE REAL-TIME PCR

Total RNA was isolated using Trizol (invitrogen) following the manufacturer's instructions, and 0.5 μg of total RNA was reverse-transcribed into cDNA. Polymerase chain reaction (PCR) amplifications were performed with the exTaq polymerase (Takara). Sequences of all primers are listed in Table I. For the quantitative RT-PCR (qRT-PCR), HS3ST3B1 was amplified using the SYBR® Premix Ex Taq TM (Takara, Japan) in a 10 μl reaction volume on an Applied Biosystems 7500 Fast Real-Time PCR System (Carlsbad, CA). 18s rRNA was used as an internal control.

WESTERN BLOT

Total proteins were extracted and the concentration was determined using the bicinchoninic acid protein assay kit (Beyotime). The total

TABLE I. Human Specific Primer Sequences Used in PCR

Primers	Sequences (5′ to 3′)
Jagged-1 F	TGGGCTTTGAGTGTGAGTGT
Jagged-1 R	CCCCGTGGGAACAGTTATTA
Notch-1 F	CACTGTGGGCGGGTCC
Notch-1 R	GTTGTATTGGTTCGGCACCAT
VEGF F	TCGGGCCTCCGGAAACCATGA
VEGF R	CCTGGTGAGAGATCTGGTTC
HS3ST3B1 F	GCTACGACAAGGGCCTC
HS3ST3B1 R	TCAAGCTCTCGAAGGTGG
18s F	GTGGAGCGATTTGTCTGGTT
18s R	GGACATCTAAGGGCATCACAG

cellular protein extracts were separated by electrophoresis on SDS-PAGE gels and blotted onto nitrocellulose filter membranes (Millipore). The blots were incubated with antibodies against phosphoinositide 3-kinase p85 (PI3K), phospho-ERK1/2, total ERK1/2, phospho-Akt (Ser 473), phospho-Akt (Thr 308), total AKT, cleaved Notch1, Dll4, Snail (Cell Signaling Technology), Jagged-1 (abcam), Notch-1 (Invitrogen), HS3ST3B1 and β-actin (Santa Cruz). Protein bands were detected by incubation with HRP-conjugated secondary antibodies, and visualized with enhanced chemiluminescence reagent (Pierce).

NUDE MOUSE XENOGRAFTS

Thirty two male BALB/c nude mice (6 weeks of age, 18–22 g) were purchased from Vital River Laboratory Animal Technology Co. Ltd. This study was carried out in accordance with the recommendations in the Guide for the Care and Use of Laboratory Animals of the National Institutes of Health. All surgeries were performed under anesthesia with sodium pentobarbital. The mice were divided into four groups. A total of 3.5×10^6 HS3ST3B1 over-expression cells or 3×10^6 HS3ST3B1 knockdown cells in 50 μl RPMI 1640 were mixed with 250 μl ice-cold matrigel and subcutaneously inoculated on the left flank of each nude mouse. After inoculation, tumor growth was examined every 3 days by measuring the length and width with a vernier caliper and calculating tumor volumes as $0.5 \times (\text{Length} \times \text{Width} \times \text{Width})$. On day 18, the animals were euthanized, and the tumors were excised, weighed and photographed. The tumors were fixed in 10% formalin for immunohistochemistry.

IMMUNOHISTOCHEMISTRY

The tumor tissues from nude mice were embedded in paraffin and sectioned for immunohistochemical analysis. Endothelial cells were identified by immunostaining with an antibody against CD31 (abcam). Microvascular density (MVD) was calculated by quantifying CD31-positive microvessels per field of view. CD31-positive staining of vascular endothelial cells was analyzed by Image-Pro Plus software. *In vivo* detection of Notch-1 and phospho-Akt (Ser 473) expression was performed by staining tissue sections with Notch-1- and phospho-Akt (Ser 473)-specific antibodies, followed by incubation with HRP-conjugated IgG. After washing, the sections were incubated with streptavidin peroxidase, lightly counterstained with hematoxylin, and observed under a photomicroscope.

STATISTICAL ANALYSIS

The results are presented as mean values ± standard error. $P < 0.05$ was considered to be statistically significant ($^{*}P < 0.05$, $^{**}P < 0.01$ and $^{***}P < 0.001$). Statistical analyses were performed by single factor ANOVA and unpaired, two-tailed Student's *t*-test using PRISM software (GraphPad Software).

RESULTS

OVER-EXPRESSION AND KNOCKDOWN OF HS3ST3B1 IN LEUKEMIA CELLS

After puromycin selection, FACS analysis revealed GFP expression in almost 99% of the transduced cells (data not shown). RT-PCR, Western blotting and the Quantitative PCR analysis verified the efficacy of transduction by revealing markedly increased expression of HS3ST3B1 in the over-expression cells (LV-3ST3B1) versus the cells containing the LV empty vector (LV-vector), and a significantly reduced expression in the HS3ST3B1 knockdown cells (LV-sh3ST3B1, U937 cells expressing HS3ST3B1-shRNA) compared with the cells that were transduced with the scrambled shRNA (LV-scrambled) (Fig. 1A–C).

HS3ST3B1 PROMOTED LEUKEMIA CELL PROLIFERATION

We first used the MTT assay to determine whether HS3ST3B1 expression affected U937 cell proliferation. The proliferation rate was presented as proliferation fold change over LV-vector or LV-scrambled cells. After 48 h, there was a significant increase in the proliferation of the HS3ST3B1 over-expression cells compared with that of the LV-vector cells, while HS3ST3B1 knockdown led to a 26.4% inhibition of cell proliferation compared with the scrambled shRNA control (Fig. 1D).

The effect of HS3ST3B1 on U937 cell growth was also confirmed by the colony formation assay. In the soft agar colony formation assay, there was a 25.7% increase in colony number and a 29.4% increase in colony size for the HS3ST3B1 over-expression cells compared with the LV-vector cells at day 10. In contrast, the HS3ST3B1 knockdown cells formed smaller and fewer colonies than the LV-scrambled cells at the same time point (Fig. 1E,F).

Collectively, our results demonstrated that HS3ST3B1 promoted U937 cell proliferation and colony formation.

HS3ST3B1 EXPRESSION IN LEUKEMIA CELLS INDUCED HUVEC MIGRATION AND TUBE FORMATION IN VITRO

HS3ST3B1 expression did not confer a growth advantage to human umbilical vein endothelial cells (HUVECs) (data not shown). Next we asked if conditioned medium (CM) from leukemia cell culture could affect other cellular behaviors of HUVECs. In the wound-healing assay, CM from the HS3ST3B1 over-expression U937 cells significantly enhanced HUVEC migration by 59% compared with the control, as quantified by measuring the area of the wound during the "wound healing" process (Fig. 2A). By comparison, the addition of LV-sh3ST3B1 CM significantly reduced HUVEC migration by 37% compared with the treatment by LV-scrambled CM (Fig. 2B). In the tube formation assay, the CM

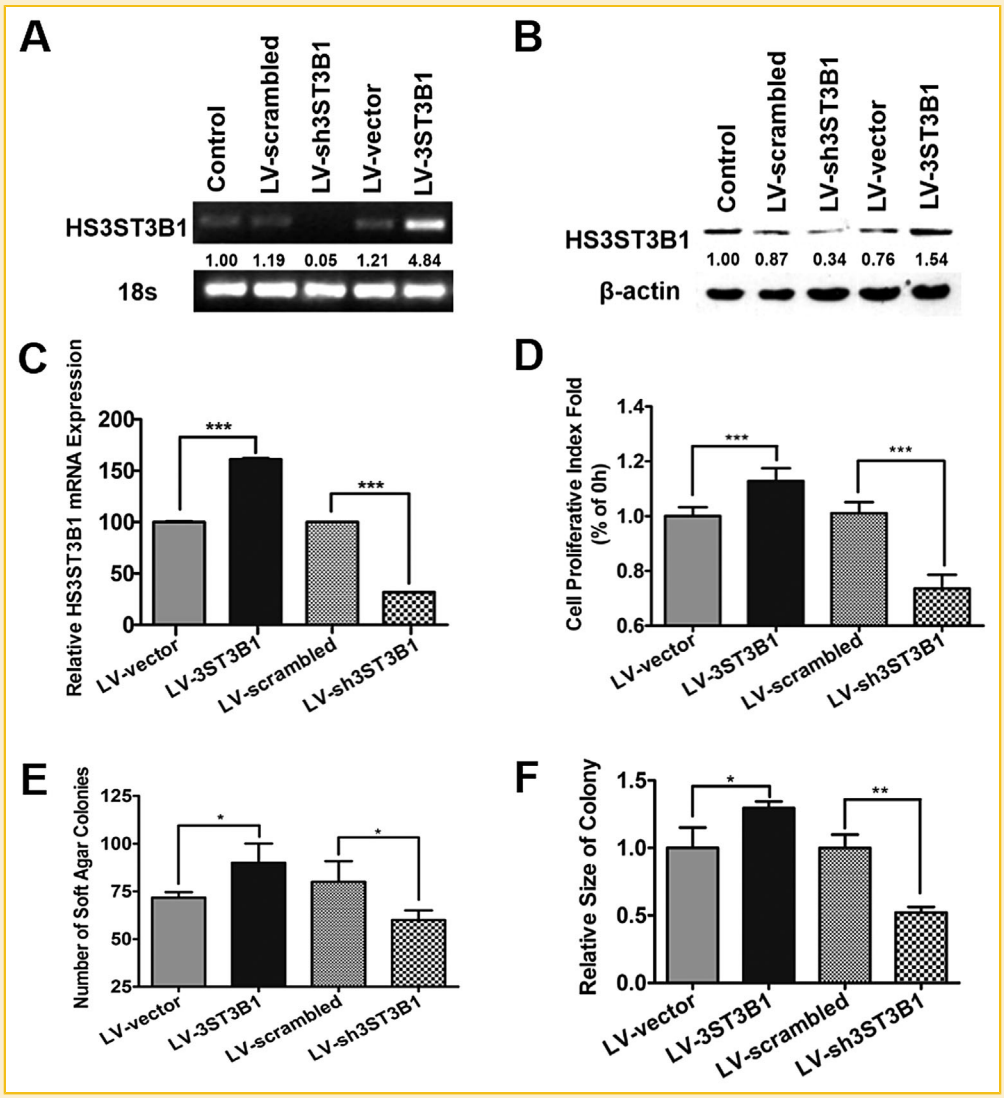

Fig. 1. HS3ST3B1 expression promoted acute myeloid leukemia cell proliferation and colony formation. A,B: U937 cells, either un-transduced (Control) or transduced with scrambled shRNA (LV-scrambled) or 3ST3B1 shRNA (LV-sh3ST3B1) or empty vector (LV-vector) or HS3ST3B1 full length plasmid, were assessed for HS3ST3B1 mRNA (A) or protein (B) expression. C: HS3ST3B1 mRNA measured by Quantitative RT-PCR relative to 18 s rRNA in U937 stable transduced cells. D: HS3ST3B1 affected U937 cells proliferation. HS3ST3B1 over-expression or knockdown cells were cultured for 48 h then cell proliferation was determined by MTT assay. Data are shown as mean fold changes in cell proliferation compared to empty vector or scrambled shRNA cells. E,F: HS3ST3B1 induced U937 cells colony formation. HS3ST3B1 over-expression or knockdown cells were planted on soft agar and cultured for 10 days, and the colony formation was quantified by number of colonies and the average colony size. Results are presented as mean ± S.D. of three independent experiments. Error bars represent S.D. of three independent experiments. $^{*}P < 0.05$, $^{**}P < 0.01$, $^{***}P < 0.001$ as determined by an unpaired Student's *t*-test.

from the HS3ST3B1 over-expression cells promoted the development of 1.8-fold more tubules than the CM of the LV-vector-transduced cells. Notably, the HS3ST3B1 knockdown CM reduced tube formation to 46% compared with the scrambled control (Fig. 2C,D). Taken together, our results support that HS3ST3B1 promotes angiogenesis.

HS3ST3B1 INCREASED VEGF EXPRESSION AND RELEASE BY LEUKEMIA CELLS

The following experiments were designed to investigate how altered HS3ST3B1 expression affected the angiogenesis *in vitro*.

We found that the VEGF mRNA expression was up-regulated in the HS3ST3B1 over-expression U937 cells and down-regulated in the HS3ST3B1 knockdown U937 cells (Fig. 3A). We therefore determined whether VEGF protein expression and secretion into culture medium correlated with HS3ST3B1 expression level. The ELISA results demonstrated that the CM from HS3ST3B1 over-expression cells was enriched with 30% more VEGF protein compared with the CM from control cells. Conversely, the HS3ST3B1 knockdown cells secreted 13.6% less VEGF than the LV-scrambled cells (Fig. 3B). Notably, cytoplasmic VEGF level remained constant regardless of the HS3ST3B1 expression level (Fig. 3C). These data

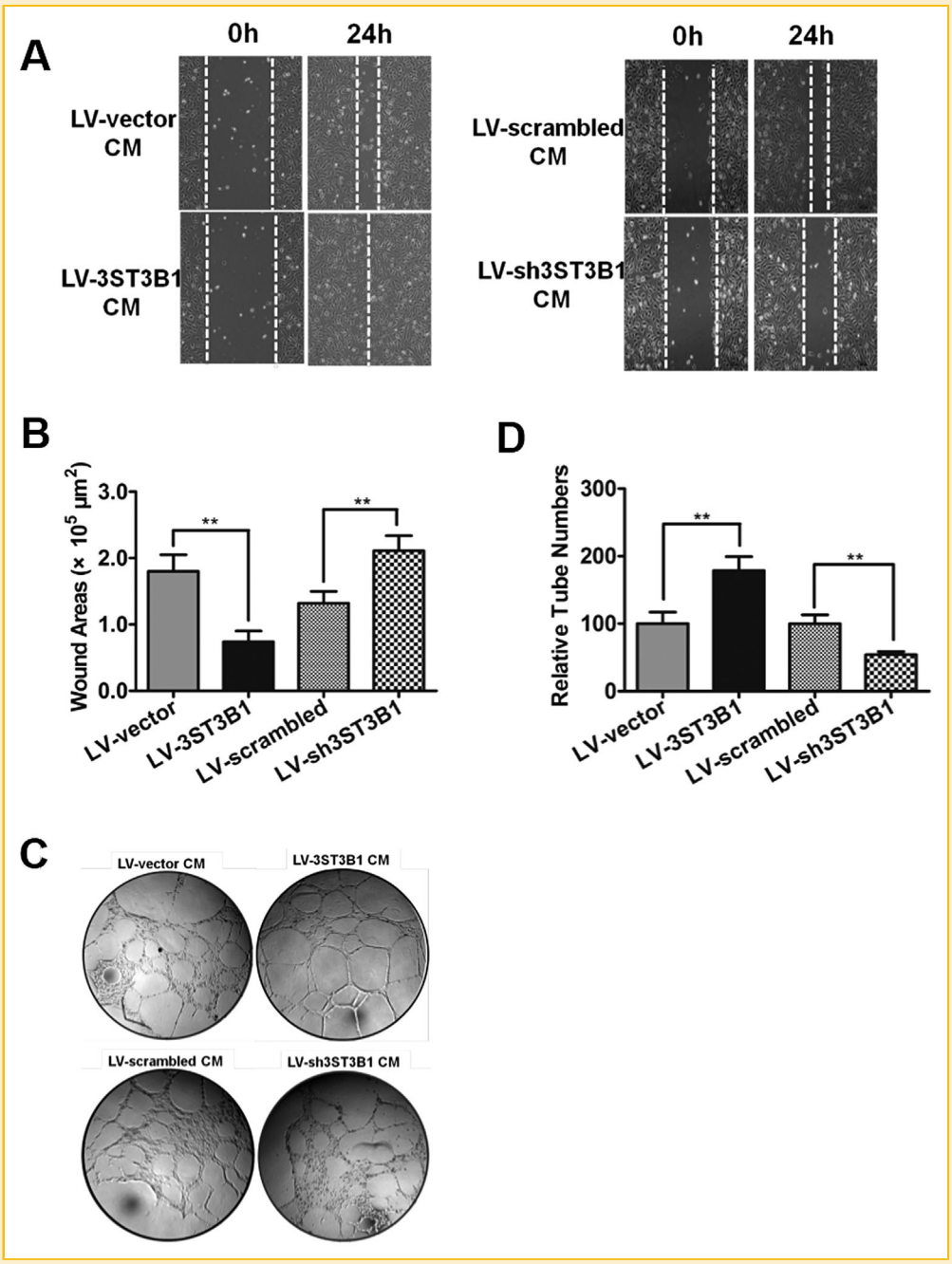

Fig. 2. HS3ST3B1 expression in leukemia cells induced HUVEC migration and tube formation (angiogenesis). A: HS3ST3B1 expression level affected the induction of HUVEC lateral migration by U937-conditioned medium. Each HUVEC monolayer was scraped to generate a wound ($t = 0$ h), and the cells were then incubated with conditioned medium from the HS3ST3B1 over-expression or knockdown cells. After 24 h, the cells were imaged at 100 × magnification. The wound areas at time 0 and 24 are indicated by dotted lines. B: Quantification of the effect of HS3ST3B1 expression by U937 cells on HUVEC migration in the wound-healing assay. The experiment was performed at least 3 times and the values represent mean ± S.D. C: HS3ST3B1 expression level affected the induction of HUVEC tubular formation by U937-conditioned medium. HUVECs were cultured on growth factor reduced matrigel in 50% CM. Representative images of tube formation after 8 h of culturing are shown (40 × magnification). D: Quantitative measurement of tube formation. Each treatment was assayed at least three times, and the corresponding values (mean ± S.D.) were plotted as fold difference versus control (empty vector or scrambled shRNA). $^{*}P < 0.05$; $^{**}P < 0.01$, as determined by unpaired Student's *t*-test.

indicated that the 3-O-sulfation of HS by HS3ST3B1 facilitated VEGF shedding.

To ascertain VEGF is an important target of HS3ST3B1, we examined VEGF expression after treatment with suramin, a heparanase inhibitor [Cui et al., 2011]. Our results found that suramin markedly decreased the levels of VEGF in the culture media dose-dependently, with 200 μM suramin dramatically reducing VEGF secretion by 50% in both HS3ST3B1 over-

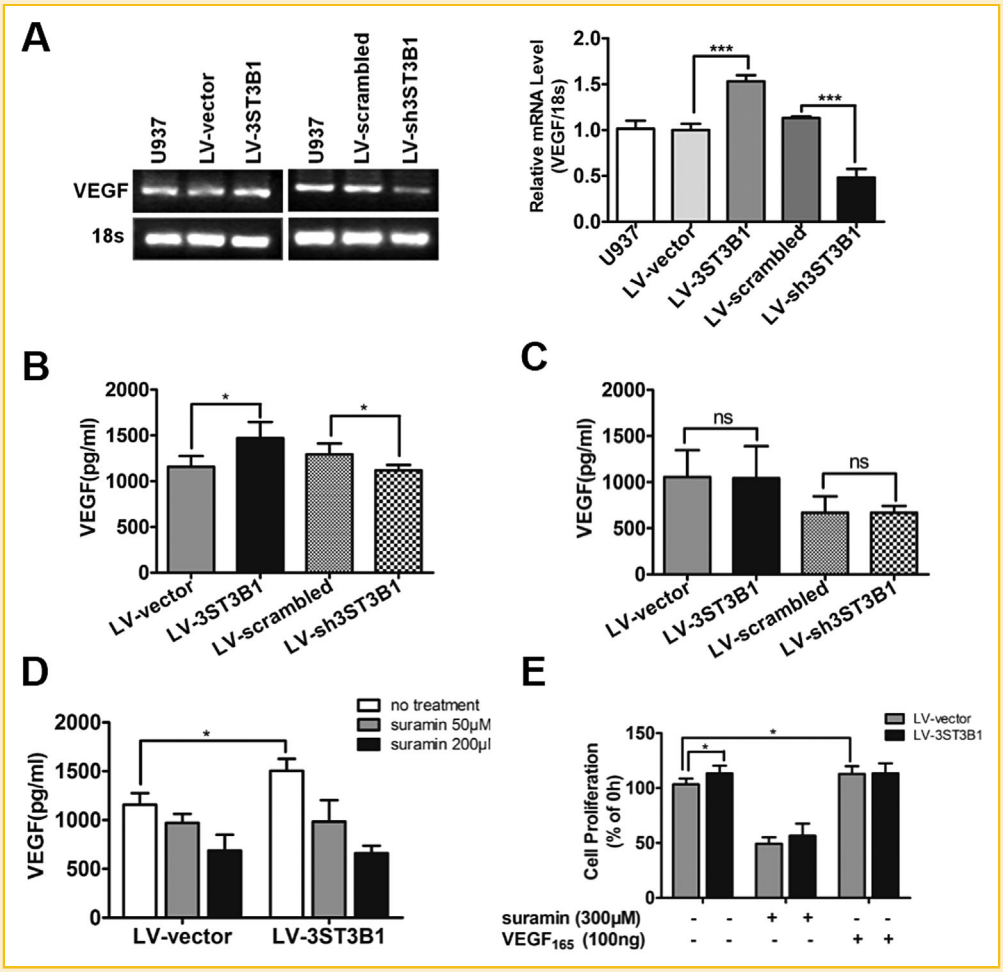

Fig. 3. The 3-O-sulfation of HS affected VEGF secretion in U937 cells. A:VEGF expression was measured by RT-PCR in U937 cells with altered HS3ST3B1 expression. 18 s rRNA served as the loading control. The right panel shows the results of the densitometric analysis. B: HS3ST3B1 expression affected VEGF secretion by U937 cells. A total of 7.5×10^5 cells were cultured in RPMI 1640 with 1% serum for 48 h. The level of VEGF in the cell medium was measured using a commercial ELISA kit. C: HS3ST3B1 expression did not affect cytosolic VEGF level in U937 cells. D: HS3ST3B1-induced secretion of VEGF was attenuated by the pan-heparanase inhibitor suramin. The level of secreted VEGF in the HS3ST3B1 over-expression and empty vector cells were measured by ELISA after incubation with or without suramin at 50 or 200 μM for 48 h in medium containing 1% serum. E: The addition of $VEGF_{165}$ promoted U937 cells proliferation to the same extent as HS3ST3B1 over-expression did. The HS3ST3B1 over-expression or empty vector cells were treated with 300 μM suramin or 100 ng/ml $VEGF_{165}$ for 24 h, and cell proliferation was evaluated by the MTT assay. Data are expressed as mean ± S.D. $^{*}P < 0.05$, $^{***}P < 0.001$; ns, no significant differences. All experiments were performed in triplicate and were repeated at least three times.

expression cells and LV-vector cells. Notably, the significant effect of HS3ST3B1 over-expression on VEGF release was diminished after suramin treatment (Fig. 3D). This result indicated that the 3-O-sulfation of HS by HS3ST3B1 facilitated heparanase-induced VEGF shedding. To further address if VEGF secretion was a direct result of the HS 3-O-sulfation in AML cells, U937 cells were treated with 25 ng $VEGF_{165}$, and cell proliferation was then analyzed by the MTT assay. The results showed that the addition of $VEGF_{165}$ had the same growth-promoting effect as HS3ST3B1 over-expression did on U937 cells, indicating that the enhanced cell proliferation that was induced by HS3ST3B1 over-expression could be due to VEGF secretion (Fig. 3E). These results supported that VEGF is indeed an important functional target of HS3ST3B1 in U937 cells.

HS3ST3B1 PROMOTED THE ACTIVATION OF THE NOTCH-1-JAGGED-1, PI3K-AKT AND ERK PATHWAYS

To delineate whether HS3ST3B1 affects the Notch-1 pathway, which is tightly linked with VEGF pathway [Liu et al., 2003], we assessed the expression levels of Notch-1 and its ligands in AML cells. The results showed that the levels of Notch-1 and one ligand Jagged-1 were positively correlated with HS3ST3B1 expression level (Fig. 4A, B); another ligand Dll4 expression did not reveal much changes (Figure S1). We also found that the protein level of the Notch intracellular domain (NICD) was down-regulated in the HS3ST3B1 knockdown U937 cells but up-regulated in the HS3ST3B1 over-expression U937 cells, which directly reflected that HS3ST3B1 can activate Notch1 signaling (Fig. 4C). Snail is known to be specifically associated with Jagged1-mediated Notch activation and has been

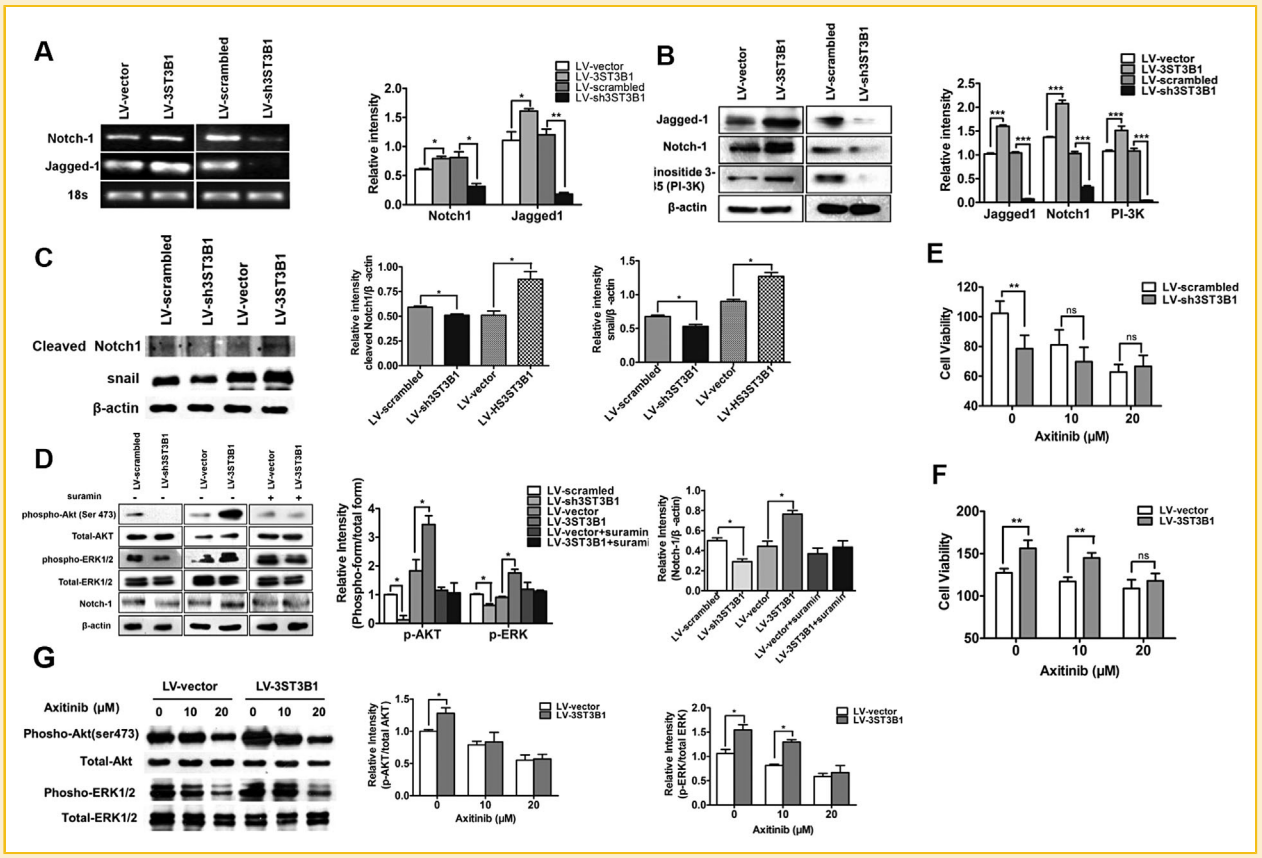

Fig. 4. The PI3K-AKT and ERK signaling pathways are essential for VEGF induction by HS3ST3B1. A: The expression of Notch-1 and Jagged-1 was increased in the HS3ST3B1 over-expression cells and reduced in the HS3ST3B1 knockdown cells. The mRNA level was detected by RT-PCR with 18 s as the internal control. The right panel shows the densitometric analysis. B: HS3ST3B1 expression affected the expression of Notch-1, Jagged-1, and phosphorylated PI3K in the HS3ST3B1 over-expression or knockdown cells. Protein expression levels were measured by western blot with anti-Notch-1, anti-Jagged-1, and anti-PI3K (p85) antibodies. β-actin was blotted as a loading control. The right panel shows the densitometric analysis. C: HS3ST3B1-induced Notch1 signaling activation. The levels of cleaved Notch1 and Snail were measured by western blot with anti-cleaved Notch1 and anti-Snail antibodies. Representative results are shown along with densitometric analysis showing the fold change of protein levels in U937 cells expressing different levels of HS3ST3B1. β-actin was blotted as the internal control. D: HS3ST3B1 induced the expression of Notch-1, phosphorylation of AKT and ERK, which was reversible by the pan-heparanase inhibitor suramin. The expression of Notch-1, AKT and ERK in the HS3ST3B1 over-expression and knockdown cells as well as in the suramin-treated (50 μM) HS3ST3B1 over-expression cells were measured by western blot with anti-Notch-1, anti-AKT, anti-phospho-AKT (Ser473), anti-ERK1/2 and anti-phospho-ERK1/2 antibodies. β-actin was blotted as a loading control. The middle and right panel shows the densitometric analysis. E,F: The VEGFR inhibitor axitinib attenuated the growth-promoting effect of HS3ST3B1. The U937 stably transduced cells were treated with 10 or 20 μM axitinib for 24 h, and cell proliferation was evaluated by the MTT assay. G: Axitinib treatment blocked HS3ST3B1-induced activation of signaling pathways. The HS3ST3B1 over-expression cells were treated with 10 or 20 μM axitinib, followed by western blot. The right panel shows the densitometric analysis. Data are expressed as mean ± S.D. $^{*}P < 0.05$; $^{**}P < 0.01$; $^{***}P < 0.001$; ns, no significant differences.

reported as a downstream target of Notch signaling in cancer [Leong et al., 2007; Wang et al., 2012]. Consistently, we found that Snail was down-regulated in the HS3ST3B1 knockdown U937 cells but up-regulated in the HS3ST3B1 over-expression U937 cells (Fig. 4C).

Next, we sought to determine if HS3ST3B1 affects ERK1/2 and AKT signalings, which are downstream targets for both VEGF and Notch-1 pathways [Fitzgerald et al., 2000; Hayashi and Kume, 2008]. We found that HS3ST3B1 positively regulated ERK1/2 phosphorylation and AKT phosphorylation at serine 473 (Fig. 4D). The heparanase inhibitor suramin significantly inhibited VEGF secretion, and suramin also blocked VEGF-induced activation of Notch-1, ERK and AKT (Fig. 4D). To confirm that HS3ST3B1 positively contributed to AML progression through the induction of VEGF and that ERK and AKT phosphorylation was downstream of VEGF activation, we used the VEGFR inhibitor axitinib to block VEGF function [Adomako-Ankomah and Ettensohn, 2013]. In the MTT assay, the HS3ST3B1 stably transduced cells were treated with 10 or 20 μM axitinib, the results showed that the addition of the VEGFR inhibitor decreased cells proliferation; moreover, the inhibitory effect was more significant in the HS3ST3B1 high expression cells. This result indicates that the HS3ST3B1 expression-induced cell proliferation was indeed due to VEGF secretion (Fig. 4E,F). When the HS3ST3B1 over-expression cells were treated with axitinib, there was a significant decrease in ERK1/2 and AKT phosphorylation, and the axitinib can attenuate the different expression resulted from HS3ST3B1 overexpression (Fig. 4G). These results supported the

hypothesis that the expression of HS3ST3B1 induces VEGF-mediated activation of ERK and AKT signaling. Taken together, our findings indicate a relationship between HS3ST3B1 and the VEGF-activated signaling pathways.

HS3ST3B1 AUGMENTED TUMOR GROWTH AND ANGIOGENESIS IN A XENOGRAFT MOUSE MODEL

To examine the effects of HS3ST3B1 on the tumorigenicity and angiogenesis of U937 cells *in vivo*, we assessed tumor growth and angiogenesis in immunocompromised nude mice. Tumor size was monitored every three days by a vernier caliper, and we found that the tumors from the HS3ST3B1 over-expression group were significantly larger than those from the LV-vector group ($359.2\,mm^3$ (over-expression) vs. $252.1\,mm^3$ (vector), $P < 0.01$) (Fig. 5A). At the end of the experiment, the mice were euthanized and the tumors were weighed. The excised tumors from the HS3ST3B1 over-expression group were much larger and heavier than those from the LV-vector group.

In contrast, a marked reduction in the tumor growth rate and tumor weight was observed in the HS3ST3B1 knockdown group compared with the LV-scrambled group (Fig. 5C,D). In addition, there were no differences in the mouse body weight amongst the groups (Fig. 5E,F). Figure 5G showed the HS3ST3B1 expression in xenografts.

When we analyzed the expression of Notch-1 and p-AKT in the U937-derived tumors by IHC staining, we found increased expression of both proteins in the HS3ST3B1 over-expression group compared with the LV-vector group. In addition, we observed an overall decrease in AKT phosphorylation and Notch-1 expression in the tumor tissues from the HS3ST3B1 knockdown group (Fig. 6A–D). Furthermore, we assessed microvessel formation in the xenografts by staining for the endothelial marker CD31, and we found that the average microvessel number in the xenografts of the HS3ST3B1 over-expression cells was significantly higher than in the xenografts of the LV-scrambled cells; in contrast, microvessels were barely detected in the xenografts of the HS3ST3B1 knockdown cells (Fig. 6E). These findings strongly suggested that HS3ST3B1 promoted an angiogenic response *in vivo*.

DISCUSSION

VEGF is an essential regulator of physiological and pathological angiogenesis, and it has also been shown to trigger the growth, survival and migration of leukemia cells [Ferrara, 2000]. VEGF/VEGFRs act in an autocrine or paracrine manner on endothelial cells as well as certain malignant cells [Santos and Dias, 2004]. Increased VEGF production by tumor cells and higher microvessel density are highly correlated with adverse clinical outcome of AML [Padro et al., 2000; de Bont et al., 2001; Shih et al., 2006]. A number of *in vitro* and *in vivo* studies have examined the role of HSPG in modulation of VEGF activity, and the interaction of HS with HS-binding growth factors is thought to be dependent on the patterns of the sulfate and hexuronic acid isoform residues [Sasisekharan et al., 2002; Bishop et al., 2007; Zhang, 2010]. These studies allowed us to speculate that VEGF is an important functional target of HS3ST3B1. Here, we demonstrated that HS3ST3B1 effectively promoted angiogenesis and proliferation in AML through the induction of VEGF mRNA expression and protein secretion. Our results are in agreement with previous reports implicating that the binding affinity between VEGF and HS likely depends on the specific structural features of the HS oligosaccharides, including their degree of sulfation, sugar stereochemistry and conformation [Robinson et al., 2006]. However, a critical and challenging question that remains to be answered is whether and how VEGF binds to 3-O-sulfated HS.

It should be noted that AML blasts synthesize and secrete VEGF, which in turn elicits rapid and sustained AKT phosphorylation in AML cells through a PI3K-dependent mechanism. This effect of VEGF was demonstrated using the PI3K inhibitor wortmannin, which effectively blocked VEGF-induced AKT phosphorylation [List et al., 2004]. We confirmed this finding in our study and found that the level of p-AKT (ser473) was significantly decreased in the HS3ST3B1 knockdown cells and elevated in the HS3ST3B1 over-expression cells in comparison with the corresponding controls. We also found that there was no significant difference in the phosphorylation level of AKT Thr308 when HS3ST3B1 expression was altered, suggesting that HS3ST3B1 expression was specifically correlated with Ser473 but not Thr308 phosphorylation on AKT (Figure S2). ERK1/2 is also activated by growth factors, such as VEGF, which leads to increased cell growth, differentiation and migration [Casalou et al., 2007]. In this study we found the level of ERK phosphorylation was also correlated with HS3ST3B1 expression level. The ERK and AKT signaling pathways coordinate the cellular responses to a variety of extracellular stimuli [Steelman et al., 2011] and play critical roles in cell proliferation, survival, migration and differentiation [Gan et al., 2010; Huynh et al., 2010; Cheng et al., 2011]. VEGF is a heparin-binding angiogenic growth factor, and the heparanase enzyme could cleave heparan sulfate and release fragments that are 10–20 sugar residues long. The shedding of active HS-bound VEGF and the release of HS degradation fragments promote VEGF-receptor (VEGFR) binding, dimerization, and signaling [Kato et al., 1998; Elkin et al., 2001; Bitan et al., 2002; Vlodavsky and Friedmann, 2001]. Our results strongly suggest that 3-O-sulfation of HS facilitated heparanase-mediated VEGF shedding in AML cells: Inhibition of heparanase by suramin potently prevented VEGF secretion, subsequently blocked VEGF-induced activation of ERK and AKT. Similarly, ERK and AKT activation was also blocked when treated with the VEGFR inhibitor axitinib. We thus postulated that autocrine and/or paracrine signaling by VEGF might augment the PI3K/AKT axis and that HS3ST3B1 might facilitate this signaling cascade.

Acute myelogenous leukemia (AML) is characterized by the overexpression of Jagged-1 and Notch-1. Aberrant Jagged-1-Notch-1 signaling has been postulated to promote the development of AML by inducing excessive self-renewal with a concomitant inhibition of cell differentiation [Tohda and Nara, 2001; Chiaramonte et al., 2005]. In addition, *Drosophila* 3ST3 has a role in regulating Notch signaling, as demonstrated by the reduction in Notch signaling and the induction of neurogenic phenotypes after HS3ST-B function was blocked via transgenic RNA interference [Kamimura et al., 2004]. These data suggest that HS3ST regulates Notch signaling. Consistent with previous findings, our study also

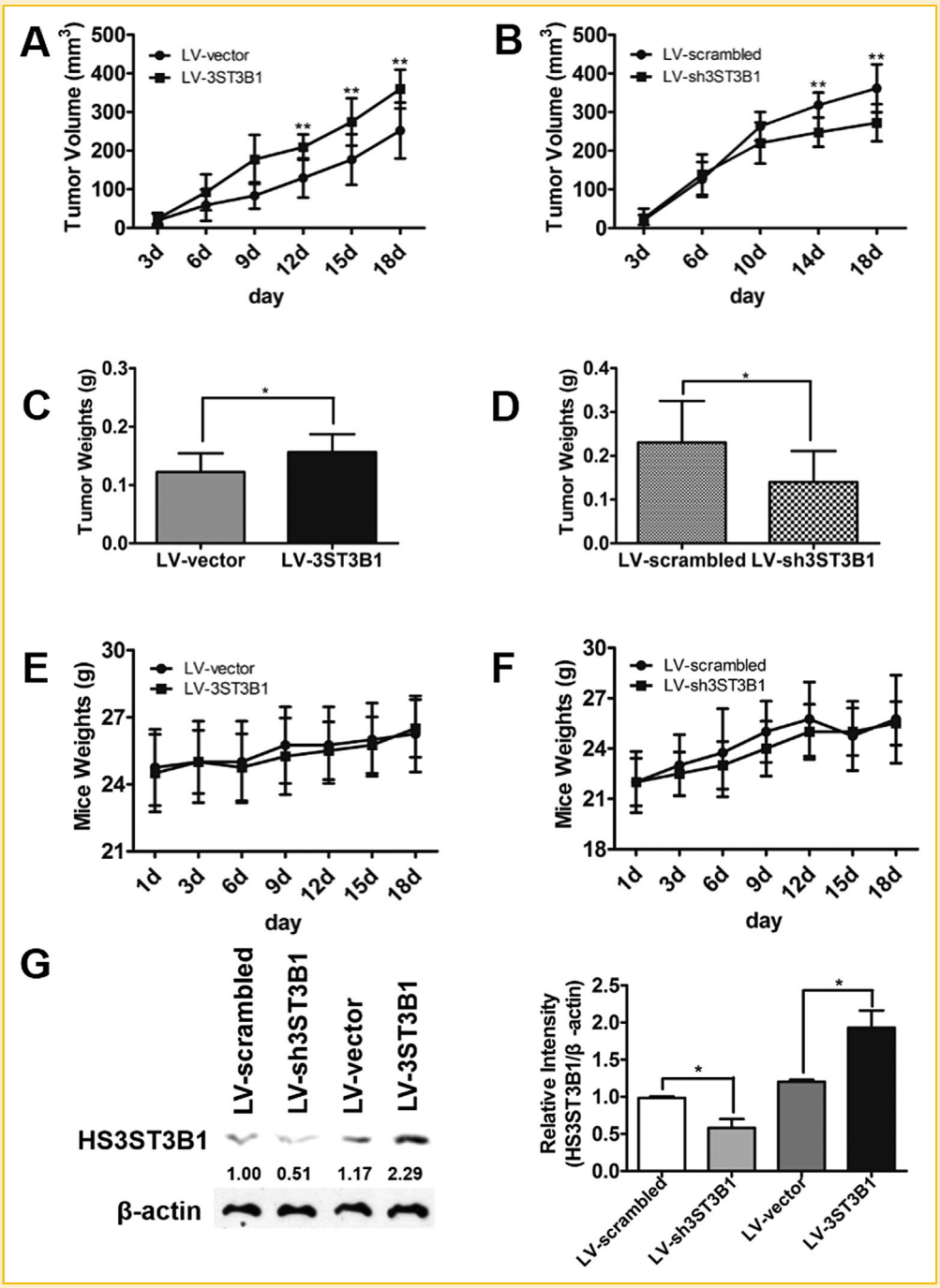

Fig. 5. HS3ST3B1 promoted tumorigenicity *in vivo*. A,B: The expression levels of HS3ST3B1 correlated with the sizes of U937 xenograft tumors. A total of 3.5×10^6 HS3ST3B1 over-expression cells or 3×10^6 HS3ST3B1 knockdown cells in 50 μl RPMI 1640 were mixed with 250 μl ice-cold matrigel and then implanted subcutaneously into the flank of each BALB/c nude mouse (8 mice/group). The mice were sacrificed after 18 days and the primary tumors were removed. The tumor growth curves indicate the mean tumor volumes (mean ± S.D.) of the HS3ST3B1 over-expression and knockdown groups. C,D: Excised tumors of the HS3ST3B1 over-expression and knockdown groups were weighed after imaging. The data are presented as mean ± S.D. E,F: Body weight changes of the HS3ST3B1 over-expression and knockdown groups during the 18 days of study. G: HS3ST3B1 and β-actin expression in xenografts were analyzed by western blotting. Representative Western blotting result with densitometric analysis showed the fold change of HS3ST3B1 protein levels in xenografts, β-actin was used as the internal control. Right panel is the statistic results. $^{*}P < 0.05$; $^{**}P < 0.01$.

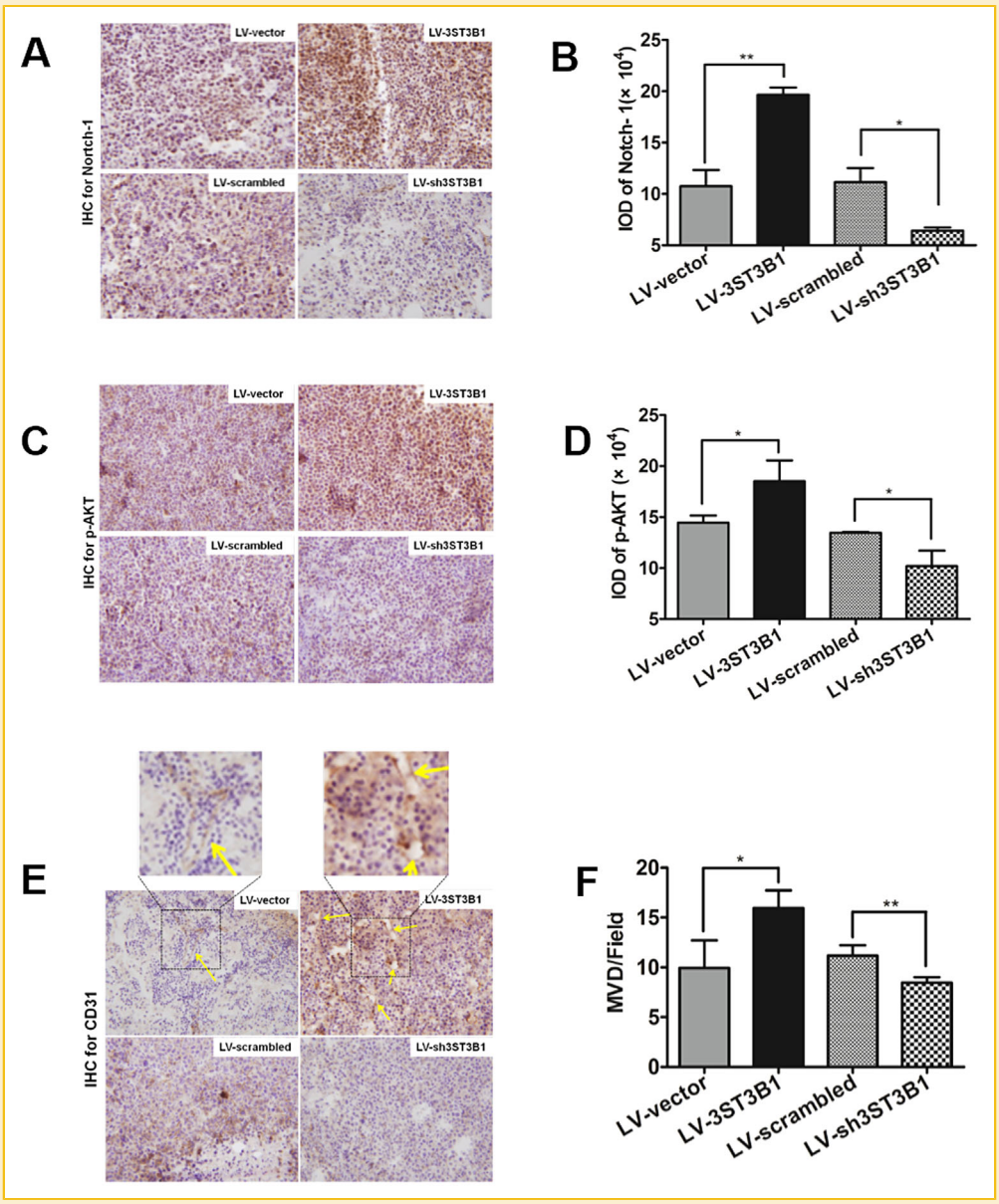

Fig. 6. Intratumoral expression of Notch-1, p-AKT and the angiogenesis marker CD31. A: Immunohistochemical analysis of Notch-1 protein levels in the HS3ST3B1 over-expression or knockdown cell xenograft tumors. B: Mean integrated optical density of Notch-1 staining. C: The expression of p-AKT was compared between the HS3ST3B1 over-expression and knockdown groups via IHC staining. D: Mean integrated optical density of p-AKT staining. E: Representative images from the immunohistochemical analysis of CD31 (endothelial marker for angiogenesis) expression in tumor sections from the HS3ST3B1 over-expression or knockdown tumors. Arrows indicate CD31-positive vessels. F: Microvascular counting was performed at 200 × magnification using Imagepro Plus. Results are presented as means ± S.D. $^{*}P < 0.05$; $^{**}P < 0.01$.

demonstrates elevated expression of Notch-1 and Jagged-1 in the HS3ST3B1 over-expression cells compared with the LV-vector cells. Importantly, increased Notch-1 and Jagged-1 expression was accompanied by enhanced expression of the Notch-1 target gene Snail and the NICD, which is the cleaved and active form of Notch-1. Furthermore, previous studies revealed that Notch-1 induces activation of the PI3K/AKT signaling pathway and that this regulatory circuitry is evolutionarily conserved from Drosophila to humans [Palomero et al., 2008]. Collectively, data from the current study demonstrate a functional link between HS3ST3B1 and the Notch, MAPK, and PI3K-AKT pathways and provide a possible mechanism for the HS3ST3B1-induced, VEGF-dependent proliferation of AML cells (Fig. 7).

In summary, we describe an important role of HS3ST3B1 in regulating different aspects of AML pathology, and these effects could exacerbate the malignancy of AML cells *in vivo*. Therefore, HS3ST3B1 may be a potential therapeutic target in AML patients.

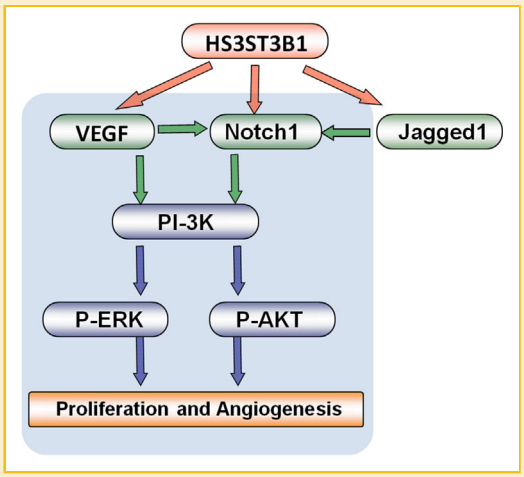

Fig. 7. Schematic diagram of HS3ST3B1-regulated VEGF and Notch-1 signaling.

ACKNOWLEDGEMENTS

This work was supported by the Funds for Creative Research Groups of China, National Natural Science Foundation of China (No. 81421005); the Priority Academic Program Development of Jiangsu Higher Education Institutions (PAPD); and the New Century 623 Excellent Talents in University (NCET-12-0976)

REFERENCES

Adomako-Ankomah A, Ettensohn CA. 2013. Growth factor-mediated mesodermal cell guidance and skeletogenesis during sea urchin gastrulation. Development 140:4214–4225.

Bellamy WT, Richter L, Sirjani D, Roxas C, Glinsmann-Gibson B, Frutiger Y, Grogan TM, List AF. 2001. Vascular endothelial cell growth factor is an autocrine promoter of abnormal localized immature myeloid precursors and leukemia progenitor formation in myelodysplastic syndromes. Blood 97:1427–1434.

Bishop JR, Schuksz M, Esko JD. 2007. Heparan sulphate proteoglycans fine-tune mammalian physiology. Nature 446:1030–1037.

Bitan M, Polliack A, Zecchina G, Nagler A, Friedmann Y, Nadav L, Deutsch V, Pecker I, Eldor A, Vlodavsky I, Katz BZ. 2002. Heparanase expression in human leukemias is restricted to acute myeloid leukemias. Exp Hematol 30:34–41.

Casalou C, Fragoso R, Nunes JF, Dias S. 2007. VEGF/PLGF induces leukemia cell migration via P38/ERK1/2 kinase pathway, resulting in Rho GTPases activation and caveolae formation. Leukemia 21:1590–1594.

Cheng SP, Yin PH, Hsu YC, Chang YC, Huang SY, Lee JJ, Chi CW. 2011. Leptin enhances migration of human papillary thyroid cancer cells through the PI3K/AKT and MEK/ERK signaling pathways. Oncol Rep 26: 1265–1271.

Chiaramonte R, Basile A, Tassi E, Calzavara E, Cecchinato V, Rossi V, Biondi A, Comi P. 2005. A wide role for NOTCH1 signaling in acute leukemia. Cancer Lett 219:113–120.

Cui H, Shao C, Liu Q, Yu W, Fang J, Ali A, Ding K. 2011. Heparanase enhances nerve-growth-factor-induced PC12 cell neuritogenesis via the p38 MAPK pathway. Biochem J 440:273–282.

Dias S, Hattori K, Zhu Z, Heissig B, Choy M, Lane W, Wu Y, Chadburn A, Hyjek E, Gill M, Hicklin DJ, Witte L, Moore MA, Rafii S. 2000. Autocrine stimulation of VEGFR-2 activates human leukemic cell growth and migration. J Clin Invest 106:511–521.

Dong X, Han ZC, Yang R. 2007. Angiogenesis and antiangiogenic therapy in hematologic malignancies. Crit Rev Oncol Hematol 62:105–118.

Elkin M, Ilan N, Ishai-Michaeli R, Friedmann Y, Papo O, Pecker I, Vlodavsky I. 2001. Heparanase as mediator of angiogenesis: Mode of action. FASEB J 15:1661–1663.

Ferrara N. 2000. Vascular endothelial growth factor and the regulation of angiogenesis. Recent Prog Horm Res 55:15–35discussion 35-36.

Ferreras C, Rushton G, Cole CL, Babur M, Telfer BA, van Kuppevelt TH, Gardiner JM, Williams KJ, Jayson GC, Avizienyte E. 2012. Endothelial heparan sulfate 6-O-sulfation levels regulate angiogenic responses of endothelial cells to fibroblast growth factor 2 and vascular endothelial growth factor. J Biol Chem 287:36132–36146.

Fitzgerald K, Harrington A, Leder P. 2000. Ras pathway signals are required for notch-mediated oncogenesis. Oncogene 19:4191–4198.

Gan Y, Shi C, Inge L, Hibner M, Balducci J, Huang Y. 2010. Differential roles of ERK and Akt pathways in regulation of EGFR-mediated signaling and motility in prostate cancer cells. Oncogene 29:4947–4958.

Hayashi H, Kume T. 2008. Foxc transcription factors directly regulate Dll4 and Hey2 expression by interacting with the VEGF-Notch signaling pathways in endothelial cells. PLoS ONE 3:e2401.

Huynh N, Liu KH, Baldwin GS, He H. 2010. P21-activated kinase 1 stimulates colon cancer cell growth and migration/invasion via ERK- and AKT-dependent pathways. Biochim Biophys Acta 1803:1106–1113.

Kamimura K, Rhodes JM, Ueda R, McNeely M, Shukla D, Kimata K, Spear PG, Shworak NW, Nakato H. 2004. Regulation of Notch signaling by Drosophila heparan sulfate 3-O sulfotransferase. J Cell Biol 166:1069–1079.

Kato M, Wang H, Kainulainen V, Fitzgerald ML, Ledbetter S, Ornitz DM, Bernfield M. 1998. Physiological degradation converts the soluble syndecan-1 ectodomain from an inhibitor to a potent activator of FGF-2. Nat Med 4: 691–697.

Leong KG, Niessen K, Kulic I, Raouf A, Eaves C, Pollet I, Karsan A. 2007. Jagged1-mediated Notch activation induces epithelial-to-mesenchymal transition through Slug-induced repression of E-cadherin. J Exp Med 204:2935–2948.

Lindahl U, Backstrom G, Thunberg L, Leder IG. 1980. Evidence for a 3-O-sulfated D-glucosamine residue in the antithrombin-binding sequence of heparin. Proc Natl Acad Sci USA 77:6551–6555.

List AF, Glinsmann-Gibson B, Stadheim C, Meuillet EJ, Bellamy W, Powis G. 2004. Vascular endothelial growth factor receptor-1 and receptor-2 initiate a phosphatidylinositide 3-kinase-dependent clonogenic response in acute myeloid leukemia cells. Exp Hematol 32:526–535.

Liu ZJ, Shirakawa T, Li Y, Soma A, Oka M, Dotto GP, Fairman RM, Velazquez OC, Herlyn M. 2003. Regulation of Notch1 and Dll4 by vascular endothelial growth factor in arterial endothelial cells: Implications for modulating arteriogenesis and angiogenesis. Mol Cell Biol 23:14–25.

Padro T, Ruiz S, Bieker R, Burger H, Steins M, Kienast J, Buchner T, Berdel WE, Mesters RM. 2000. Increased angiogenesis in the bone marrow of patients with acute myeloid leukemia. Blood 95:2637–2644.

Palomero T, Dominguez M, Ferrando AA. 2008. The role of the PTEN/AKT Pathway in NOTCH1-induced leukemia. Cell Cycle 7:965–970.

Robinson CJ, Mulloy B, Gallagher JT, Stringer SE. 2006. VEGF165-binding sites within heparan sulfate encompass two highly sulfated domains and can be liberated by K5 lyase. J Biol Chem 281:1731–1740.

Santos SC, Dias S. 2004. Internal and external autocrine VEGF/KDR loops regulate survival of subsets of acute leukemia through distinct signaling pathways. Blood 103:3883–3889.

Sasisekharan R, Shriver Z, Venkataraman G, Narayanasami U. 2002. Roles of heparan-sulphate glycosaminoglycans in cancer. Nat Rev Cancer 2:521–528.

Shih TT, Tien HF, Liu CY, Su WP, Chan WK, Yang PC. 2006. Functional MR imaging of tumor angiogenesis predicts outcome of patients with acute myeloid leukemia. Leukemia 20:357–362.

Shworak NW, Liu J, Fritze LM, Schwartz JJ, Zhang L, Logeart D, Rosenberg RD. 1997. Molecular cloning and expression of mouse and human cDNAs encoding heparan sulfate D-glucosaminyl 3-O-sulfotransferase. J Biol Chem 272:28008–28019.

Shworak NW, Liu J, Petros LM, Zhang L, Kobayashi M, Copeland NG, Jenkins NA, Rosenberg RD. 1999. Multiple isoforms of heparan sulfate D-glucosaminyl 3-O-sulfotransferase. Isolation, characterization, and expression of human cdnas and identification of distinct genomic loci. J Biol Chem 274:5170–5184.

Song K, Li Q, Jiang ZZ, Guo CW, Li P. 2011. Heparan sulfate D-glucosaminyl 3-O-sulfotransferase-3B1, a novel epithelial-mesenchymal transition inducer in pancreatic cancer. Cancer Biol Ther 12:388–398.

Steelman LS, Chappell WH, Abrams SL, Kempf RC, Long J, Laidler P, Mijatovic S, Maksimovic-Ivanic D, Stivala F, Mazzarino MC, Donia M, Fagone P, Malaponte G, Nicoletti F, Libra M, Milella M, Tafuri A, Bonati A, Basecke J, Cocco L, Evangelisti C, Martelli AM, Montalto G, Cervello M, McCubrey JA. 2011. Roles of the Raf/MEK/ERK and PI3K/PTEN/Akt/mTOR pathways in controlling growth and sensitivity to therapy-implications for cancer and aging. Aging (Albany NY) 3:192–222.

Stone RM, O'Donnell MR, Sekeres MA. 2004. Acute myeloid leukemia. Hematology Am Soc Hematol Educ Program 2004:98–117.

Tohda S, Nara N. 2001. Expression of Notch1 and Jagged1 proteins in acute myeloid leukemia cells. Leuk Lymphoma 42:467–472.

Vanpouille C, Deligny A, Delehedde M, Denys A, Melchior A, Lienard X, Lyon M, Mazurier J, Fernig DG, Allain F. 2007. The heparin/heparan sulfate sequence that interacts with cyclophilin B contains a 3-O-sulfated N-unsubstituted glucosamine residue. J Biol Chem 282:24416–24429.

Vlodavsky I, Friedmann Y. 2001. Molecular properties and involvement of heparanase in cancer metastasis and angiogenesis. J Clin Invest 108:341–347.

Wang XQ, Zhang W, Lui EL, Zhu Y, Lu P, Yu X, Sun J, Yang S, Poon RT, Fan ST. 2012. Notch1-Snail1-E-cadherin pathway in metastatic hepatocellular carcinoma. Int J Cancer 131:E163–E172.

Zhang L. 2010. Glycosaminoglycan (GAG) biosynthesis and GAG-binding proteins. Prog Mol Biol Transl Sci 93:1–17.

de Bont ES, Rosati S, Jacobs S, Kamps WA, Vellenga E. 2001. Increased bone marrow vascularization in patients with acute myeloid leukaemia: A possible role for vascular endothelial growth factor. Br J Haematol 113:296–304.

SUPPORTING INFORMATION

Additional supporting information may be found in the online version of this article at the publisher's web-site.